

# Detecting tree crown injuries as remote sensing data anomalies

L. Gulbe <sup>1\*</sup>,

<sup>1</sup>*Space technology laboratory, Institute of Electronics and Computer Science, Riga, Latvia*

\*Contact: linda.gulbe@edi.lv

**Abstract**—The purpose of this study was to compare the anomaly detection methods with the commonly used NDVI-based approach for detecting tree crown injuries in UAV data. While dead wood was convincingly detected by both methods, Reed-Xiaoli (RX) detector provides an easier way how to label a larger variety of anomalies.

**Keywords**—anomalies, NDVI, UAV, multispectral

## I. INTRODUCTION

Tree defoliation and dechromation are two different types of tree crown injury that can be indicators of tree stress or health issues, and they are commonly monitored in tree health assessments. Defoliation refers to the loss of leaves or needles, while dechromation, on the other hand, refers to the loss of colour in leaves or needles.

Unmanned aerial vehicles (UAVs) equipped with high-resolution cameras and data processing algorithms can be used to quickly monitor defoliation and dechromation in large areas, enabling forest managers to identify and respond to emerging issues before they become severe. Since traditional methods of tree health monitoring, such as ground-based surveys, can be expensive and time-consuming, UAVs also offer a more cost-effective alternative. [1]

Various approaches can be employed to detect tree crown injuries in UAV data. Among these, the most commonly used methods are the analysis of different vegetation indices, such as NDVI [2], and the application of machine learning techniques like Random Forest or convolutional neural networks [3].

A less commonly utilised approach in processing UAV data involves the use of anomaly detection methods. Anomaly detection refers to the identification of deviations from the expected pattern or behaviour within a dataset. This approach allows for efficient data processing obtained from forest stands with varying characteristics and under different illumination conditions without the need for training datasets or additional corrections. As healthy trees are the norm in most forest stands, this method of anomaly detection can quickly and accurately identify potentially damaged areas for further investigation and management.

**The purpose of this study was to compare the effectiveness of anomaly detection methods with the commonly used NDVI-based approach for detecting tree crown injuries.**

This research was funded by the ERDF project entitled “Remote sensing based system for forest risk factor monitoring (ForestRisk)”.

## II. METHODOLOGY

### A. Study site and datasets

The methods were assessed at the study site of the Latvian State Forest Research Institute “Silava” near Valgunde, where the prevailing tree species are coniferous, namely Scots pine and Norway spruce, with a smaller fraction of deciduous trees, such as birch and alder. UAV images were captured on June 21st, 2022, with a spatial resolution of 6 cm/pixel, and for this study, RGB and NIR orthophotos were utilised.

The ground truth dataset comprises of 60 deadwood points, which were identified through visual inspection of the RGB orthophoto and tree species recorded for 582 trees using field inspection.

### B. Tree species and shadow classification

As deciduous trees make up a relatively small fraction of the study area, they need to be analysed separately to avoid mislabelling them as anomalies, as their presence would not be included in the normal patterns defined by the dominant coniferous tree species. To achieve this, coniferous and deciduous trees, along with strong shadows, were semantically segmented using the k-means method, a widely used unsupervised machine learning technique that clusters and partitions data based on similarity [4].

A spectral angle image [5] was generated by processing a colour infrared orthophoto (NIR, red, and green bands). The employed reference spectrum was an all-ones vector, and the resulting image was clustered into three clusters. The cluster with the lowest centroid values was identified as shadowed areas, while the other two clusters, representing coniferous and deciduous regions, were not labelled as such. This decision was made based on the fact that the primary objective of the algorithm was to identify prevalent patterns rather than specific class labels, as the latter were deemed unnecessary for further analysis.

### C. Anomaly detection

The Reed-Xiaoli (RX) detector is a well-known anomaly detection algorithm [6] which is particularly useful for spectral data processing.

The RX detector works by calculating the mean vector and covariance matrix of a set of pixels within a region of interest. In this study, those variables were calculated separately for coniferous and deciduous trees using semantic segmentation results from the previous step, while shadows

were not included at all. Then, for each individual pixel, the RX detector computes a scalar anomaly score based on the Mahalanobis distance between that pixel's spectral values and the mean spectral signature of pixels in the region of interest.

Coniferous/deciduous masks were not employed in the anomaly score calculation step. Instead, two anomaly score images were created: one using statistics of the coniferous trees and another using statistics of the deciduous. Resultant image *AnomalyScores* were created by applying element-wise minimum operation of those two images.

If a pixel's anomaly score in the resultant image exceeds a certain threshold, it is considered as anomaly.

For comparison purposes with anomaly scores, also Normalised Difference Vegetation Index (NDVI) images were prepared.

#### D. Anomaly thresholding

Tree crown injuries  $I$  are characterised by lower values of NDVI and higher anomaly scores:  $I_{NDVI} = NDVI \leq T_{NDVI}$  or  $I_{AnomalyScores} = AnomalyScores \geq T_{AnomalyScores}$ , where  $T_{NDVI}$  and  $T_{AnomalyScores}$  are threshold values.

In addition to the visual evaluation of different thresholds, also automated threshold estimations were performed to find the values which result in the most similar results between NDVI and RX anomalies. Overlap between pairs of  $I_{NDVI}$  and  $I_{AnomalyScores}$  were examined for all threshold combinations using pixel based Intersection over Union (IoU) as a metric. Threshold combinations were generated from range [10, 90] with step 5 for *AnomalyScores* and range [0, 0.9] with step 0.02 for *NDVI*. The IoU ranges from 0 to 1, where a score of 1 indicates a perfect overlap between the foreground pixels and a score of 0 indicates no overlap.

### III. RESULTS AND CONCLUSIONS

Table I shows the results of tree species classification. The overall accuracy (OA) of 92% can be considered as high for such a simple unsupervised approach, however, the tree species classification results could not be employed for choosing the mean vector and covariation matrix for calculating anomaly score because at pixel level accuracy is lower and would produce a lot of false positive anomalies.

TABLE I

TREE SPECIES CLASSIFICATION RESULTS. GROUND TRUTH (GT) DATA INCLUDES 530 CONIFEROUS, 52 DECIDUOUS TREES.

	Coniferous GT	Deciduous GT	User's acc.
Coniferous predicted	490	5	99%
Deciduous predicted	23	47	67.1 %
Shadow predicted	17	0	-
<b>Producer's acc.</b>	92.5%	90.4%	<b>OA=92%</b>

All dead wood samples were identified by both NDVI and *AnomalyScores* since spectral difference were very high comparing with healthy tree crowns.

Correlation analysis between NDVI and *AnomalyScores* showed no correlation with normalised correlation coefficient 0.22.

The highest IoU were 0.35 and it was achieved using  $T_{AnomalyScores} = 80$  and  $T_{NDVI} = 0.46$ .

A relatively low IoU value can be explained by the simpler thresholding of crown injuries using *AnomalyScores*. For instance, dechromated tree crowns or defoliated branches have only slightly lower NDVI values than healthy tree crowns. Meanwhile, anomaly scores have similar values for all types of anomalies and higher value differences between anomaly and healthy tree crowns, making it much easier to threshold, see examples in Fig. 1, 2.

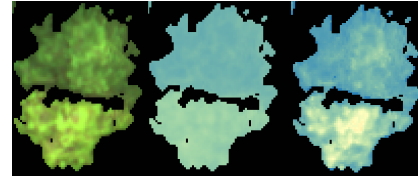


Fig. 1. From left to right: RGB image showing dechromated tree crown, NDVI, *AnomalyScores*.

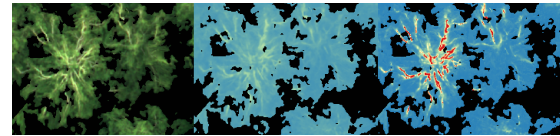


Fig. 2. From left to right: RGB image with defoliated branches, NDVI, *AnomalyScores*.

Furthermore, anomaly detectors can identify areas with unusually high NDVI values as anomalies. Therefore, anomaly detectors can provide a wider range of potential tree crown injuries, and injuries can be more easily separated from background features by thresholding.

#### ACKNOWLEDGEMENT

This research was funded by the ERDF project entitled "Remote sensing based system for forest risk factor monitoring (ForestRisk)" (Project No. 1.1.1.1/21/A/40).

#### REFERENCES

- [1] Nathalie Guimarães, Luís Pádua, Pedro Marques, Nuno Silva, Emanuel Peres, and Joaquim J Sousa. Forestry remote sensing from unmanned aerial vehicles: A review focusing on the data, processing and potentialities. *Remote Sensing*, 12(6):1046, 2020.
- [2] Adrián Cardil, Kaori Otsu, Magda Pla, Carlos Alberto Silva, and Lluís Brotons. Quantifying pine processionary moth defoliation in a pine-oak mixed forest using unmanned aerial systems and multispectral imagery. *Plos one*, 14(3):e0213027, 2019.
- [3] Lang Xia, Ruirui Zhang, Liping Chen, Longlong Li, Tongchuan Yi, Yao Wen, Chenchen Ding, and Chunxun Xie. Evaluation of deep learning segmentation models for detection of pine wilt disease in unmanned aerial vehicle images. *Remote Sensing*, 13(18):3594, 2021.
- [4] Kristina P Sinaga and Miin-Shen Yang. Unsupervised k-means clustering algorithm. *IEEE access*, 8:80716–80727, 2020.
- [5] O Abilio De Carvalho and Paulo Roberto Meneses. Spectral correlation mapper (scm): an improvement on the spectral angle mapper (sam). In *Summaries of the 9th JPL Airborne Earth Science Workshop, JPL Publication 00-18*, volume 9, page 2. JPL publication Pasadena, CA, USA, 2000.
- [6] Xinran Yu and Zhenwei Shi. Vehicle detection in remote sensing imagery based on salient information and local shape feature. *Optik*, 126(20):2485–2490, 2015.